A New Family of Sensors for Pulse Oximetry

This new family of reusable sensors for noninvasive arterial oxygen saturation measurements is designed to cover all application areas. It consists of four sensors: adult, pediatric, neonatal, and ear clip.

by Siegfried Kästle, Friedemann Noller, Siegfried Falk, Anton Bukta, Eberhard Mayer, and Dietmar Miller

Since the early 1980s, when pulse oximetry was introduced, this noninvasive method of monitoring the arterial oxygen saturation level in a patient's blood (SpO_2) has become a standard method in the clinical environment because of its simple application and the high value of the information it gives nurses and doctors. It is as common in patient monitoring to measure the oxygen level in the blood as it is to monitor heart activity with the ECG. In some application areas, like anesthesia in a surgical procedure, it is mandatory for doctors to measure this vital parameter. Its importance is obvious considering that a human being cannot survive more than five minutes without oxygen supply to the brain.

Before the advent of pulse oximetry, the common practice was to draw blood from patients and analyze the samples at regular intervals—several times a day, or even several times an hour—using large hospital laboratory equipment. These in-vitro analysis instruments were either blood gas analyzers or hemoximeters. Blood gas analyzers determine the partial pressure of oxygen in the blood (pO_2) by means of chemical sensors. Hemoximeters work on spectrometric principles and directly measure the ratio of the oxygenated hemoglobin to the total hemoglobin in a sample of blood (SaO_2).

HP pioneered the first in-vivo technology to measure a patient's oxygen saturation level without the need of drawing blood samples in 1976 with the HP 47201A eight-wavelength ear oximeter.[1] An earprobe was coupled through a fiber-optic cable to the oximeter mainframe, which contained the light source (a tungsten-iodine lamp and interference filters for wavelength selection) and receivers. This instrument served as a "gold standard" for oximetry for a long time and was even used to verify the accuracy of the first pulse oximeters in clinical studies.

The real breakthrough came in the 1980s with a new generation of instruments and sensors that were smaller in size, easier to use, and lower in cost. These new instruments used a slightly different principle from the older, purely empirical multiwavelength technology. Instead of using constant absorbance values at eight different spectral lines measured through the earlobe, the new pulse oximeters made use of the pulsatile component of arterial blood generated by the heartbeat at only two spectral lines. The necessary light was easily generated by two light-emitting diodes (LEDs) with controlled wavelengths. Small LEDs and photodiodes made it possible to mount the optical components directly on the sensor applied to the patient, avoiding the necessity of clumsy fiber-optic bundles.

Instruments and Sensors

The first pulse oximeters were standalone products. HP offered its first pulse oximetry devices as additional measurements for an existing monitoring product, the HP 78352/54 family, in 1988. A year later the Böblingen Medical Division introduced a new modular patient monitor, the Component Monitoring System,[2] for which a pulse oximeter module was also available, the HP M1020A (Fig. 1). The application was limited to adults and the only sensor available was the HP M1190A, an advanced design at that time. This sensor is the ancestor of the new sensor family presented in this paper.

Two years later, the HP 78834 neonatal monitor extended SpO_2 measurement to newborn applications. Third-party sensors were used.

Today, all typical monitoring application areas have discovered pulse oximetry: intensive care, operating rooms, emergency, patient transport, general wards, birth and delivery, and neonatal care. HP monitors serving these areas include the HP M1025A anesthetic gas monitor (1990), the HP Component Transport Monitor (1992), SpO_2 options for the HP M1722A and M1723A CodeMaster XL defibrillators (1994, Fig. 2), and recently, the HP M1205A OmniCare monitor and the HP 1350B maternal SpO_2 option for the HP XM Series fetal monitors (Fig. 3).

New SpO_2 Sensor Family

A new family of reusable HP pulse oximetry sensors is now available (Fig. 4). Lower in cost than previous reusable sensors and easier to use than adhesive disposable sensors, the new HP SpO_2 sensor family is hardware compatible with HP's installed base of pulse oximetry front ends. An upgrade to the software is necessary to update the calibration constants in the instrument algorithms to match the optical characteristics of the new sensors, such as spectra and intensity. The new

Fig. 1. *The HP M1020A SpO_2 front-end module for the HP Component Monitoring System.*

Fig. 2. *An HP CodeMaster defibrillator with SpO_2 channel.*

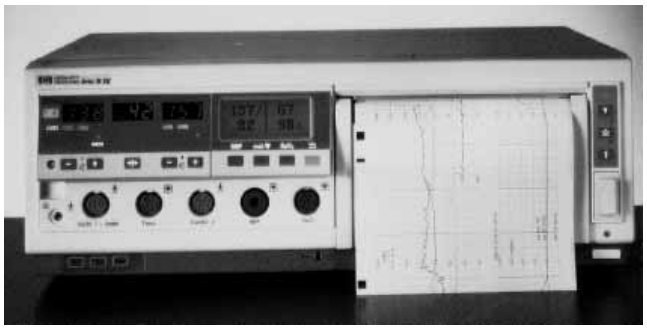

Fig. 3. *The SpO_2 channel in an HP XM Series fetal monitor monitors the mother during delivery.*

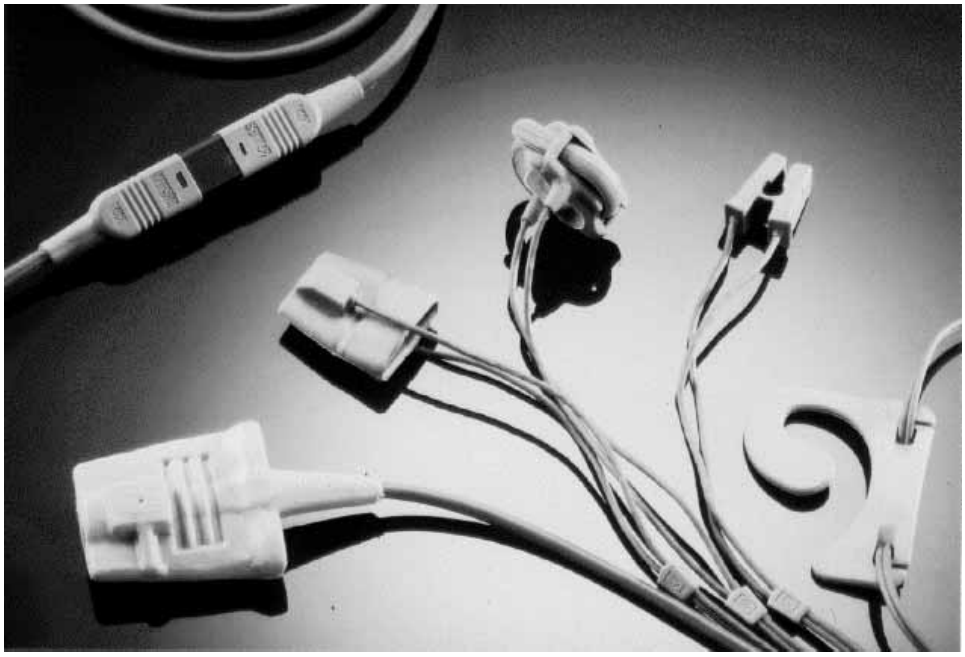

Fig. 4. *The new family of reusable HP pulse oximetry (SpO_2) sensors: (left to right) adult finger glove, pediatric finger glove, neonatal foot strap, ear clip.*

sensor family covers all application areas and consists of the HP M1191A (adult, new wavelength), M1192A (pediatric), M1193A (neonatal), and M1194A (clip).

SpO_2 Basic Measurement Principles

The breakthrough from oximetry to pulse oximetry came with the new LED technology in 1982 to 1985. LED light sources are very small and easy to drive, and have the great advantage that they can be mounted within the sensor together with a photodiode receiver (Fig. 5). For correct measurements at least two LEDs with different wavelengths are necessary. A suitable combination consists of a red LED (650 nm) and an infrared LED (940 nm). The red LED's wavelength has to be in a narrow range, which is not normally possible with standard commercially available LEDs. One way to overcome this is to provide in each sensor a calibration resistor matched to the actual LED wavelength. Another way is to select only LEDs with a fixed wavelength. This method becomes practical if the LED wafer production yields a narrow wavelength distribution. HP decided on this second method because the red LEDs could be obtained from the HP Optoelectronics Division, which had long experience in wafer production and was able to maintain a sufficiently narrow wavelength distribution.

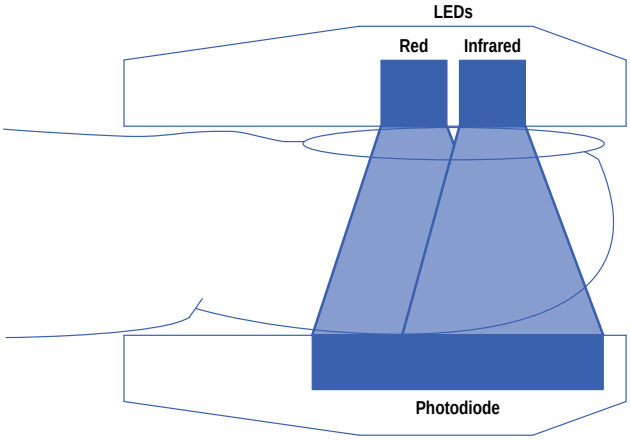

Fig. 5. *The basic components of an SpO_2 pulse oximeter sensor are two LEDs with different wavelengths as light sources and a photodiode as receiver.*

The front-end hardware applies a time multiplexed approach in which the two LEDs are switched on and off alternately. The time phases usually consist of a minimum of three: active red, active infrared, and a dark phase in which the ambient light is measured. There can be more than three phases to allow more LEDs to be powered in one multiplexing time frame or to allow additional dark phases. The phases are similar in duration. The modulation frequency (the complete frame repetition rate) typically ranges from 200 Hz to 2 kHz. The frequency spectrum of such a time multiplexed signal at the receiving photodiode consists of small bands (approximately ± 10 Hz) around the modulation frequency and its harmonics. Depending on the width of the individual LED pulses, the harmonic frequency content is of significant amplitude for several tens of harmonic orders.

For an idealized light absorbing model as shown in Fig. 6, the Lambert-Beer law applies. The intensity I of the light transmitted is related to the incident light I_0 by:

$$I = I_0 \exp(-\mathrm{Ext} \cdot c \cdot d), \qquad (1)$$

where Ext is the extinction coefficient and c is the concentration of a single light absorber with thickness d. Ext varies as a function of the absorbing substance and the wavelength of the light. Further assumptions for the validity of equation 1 are that the light source is monochromatic and has parallel propagation and that the absorber is optically homogeneous (no scattering effects).

Under these assumptions the model of Fig. 6 can be used to derive the basic pulse oximetric quantities. Fig. 7 shows a simplified model for the blood vessel system in tissue. With each heartbeat, the volume of the arteries increases before the blood is forced into the capillaries and from there into the veins. This change of arterial volume is the basis for pulse oximetry because it makes it possible to separate the arterial blood from all other absorbing substances.

Assume that there are N layers of absorbers and that the ith absorber layer has concentration c_i, thickness d_i, and extinction coefficient $\mathrm{Ext}(i,\lambda)$. From equation 1 it follows, at diastole, when there is a maximum of light intensity:

$$I_{max}(\lambda) = I_{LED}(\lambda) \exp\left(-\sum_{i=1}^{N} \mathrm{Ext}(i,\lambda) c_i d_i\right). \qquad (2)$$

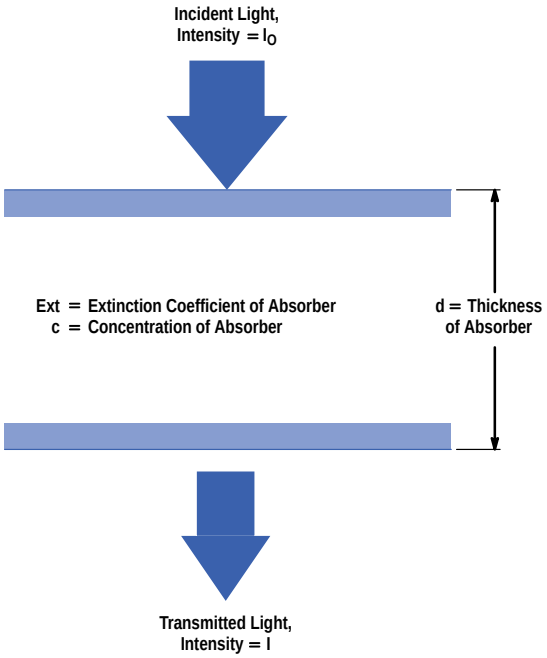

Fig. 6. *Idealized model for the validity of the Lambert-Beer law: a monochromatic light source, parallel light propagation (no point source), and no scattering.*

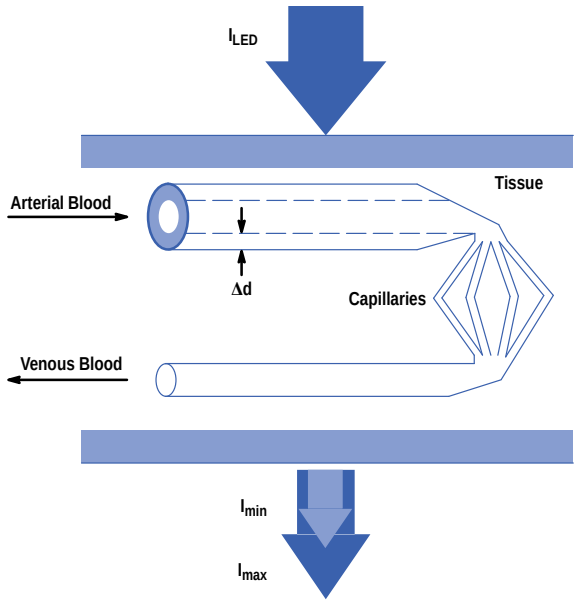

Fig. 7. *Simplified model for the blood vessel system. With each heartbeat, the arterial radius expands by an amount Δd, which yields a light intensity change from I_{max} to I_{min}.*

At systole, the maximum of the heartbeat, and under the assumption that only hemoglobin and oxyhemoglobin are active absorbers in the arterial blood, two additional absorbing parts are added in the exponent of equation 2, which yields the minimum of light intensity:

$$I_{min}(\lambda) = I_{max}(\lambda)\exp(-\Delta d(Ext(Hb,\lambda)[Hb] + Ext(HbO_2,\lambda)[HbO_2])), \quad (3)$$

where [Hb] is the concentration of hemoglobin and $[HbO_2]$ is the concentration of oxyhemoglobin. Dividing equation 2 by equation 3 and taking the logarithm yields the absorption of the arterial blood:

$$\ln\left(\frac{I_{max}(\lambda)}{I_{min}(\lambda)}\right) = \Delta d(Ext(Hb,\lambda)[Hb] + Ext(HbO_2,\lambda)[HbO_2]), \quad (4)$$

where Δd is the change in the arterial radius (see Fig. 7). The definition for the oxygen saturation in pulse oximetry is:

$$SpO_2 = \frac{[HbO_2]}{[Hb] + [HbO_2]}. \quad (5)$$

With two light sources (LEDs) of different wavelengths λ_1 and λ_2 the arterial expansion Δd can be eliminated by the following relation, which is called the *ratio*, $\mathbb{R}$:

$$\mathbb{R} = \frac{\ln\left(\frac{I_{max}(\lambda_1)}{I_{min}(\lambda_1)}\right)}{\ln\left(\frac{I_{max}(\lambda_2)}{I_{min}(\lambda_2)}\right)} = \frac{Ext(Hb,\lambda_1)(1-SpO_2) + Ext(HbO_2,\lambda_1)SpO_2}{Ext(Hb,\lambda_2)(1-SpO_2) + Ext(HbO_2,\lambda_2)SpO_2}. \quad (6)$$

Thus, the oxygen saturation SpO_2 is:

$$SpO_2 = \frac{\mathbb{R}Ext(Hb,\lambda_2) - Ext(Hb,\lambda_1)}{\mathbb{R}(Ext(Hb,\lambda_2) - Ext(HbO_2,\lambda_2)) + Ext(HbO_2,\lambda_1) - Ext(Hb,\lambda_1)}.$$

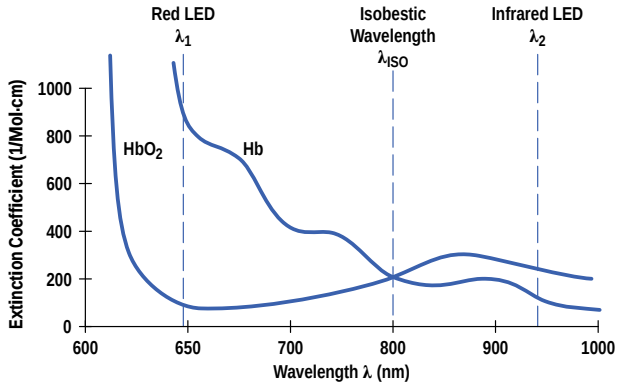

Fig. 8. *Extinction coefficients for hemoglobin Hb and oxyhemoglobin HbO_2 as a function of wavelength. A red LED with $\lambda = 650$ nm gives good resolution between HbO_2 (100% SpO_2) and Hb (0% SpO_2).*

For example, with LED wavelengths $\lambda_1 = 650$ nm and $\lambda_2 = 940$ nm,the extinction coefficients are (see Fig. 8):

$Ext(Hb,650) = 820\ (Mol \cdot cm)^{-1}$
$Ext(HbO_2,650) = 100\ (Mol \cdot cm)^{-1}$
$Ext(Hb,940) = 100\ (Mol \cdot cm)^{-1}$
$Ext(HbO_2,940) = 260\ (Mol \cdot cm)^{-1}$.

In Fig. 9 the SpO_2 is plotted as a function of the ratio $\mathbb{R}$. The Lambert-Beer relation is compared with a calibrated curve derived from real arterial blood samples from volunteers (see subarticle "**Volunteer Study for Sensor Calibration.**"). The deviations exist because conditions in the real case (complicated tissue structure, scattering effects, point light source, etc.) are different from the Lambert-Beer assumptions.

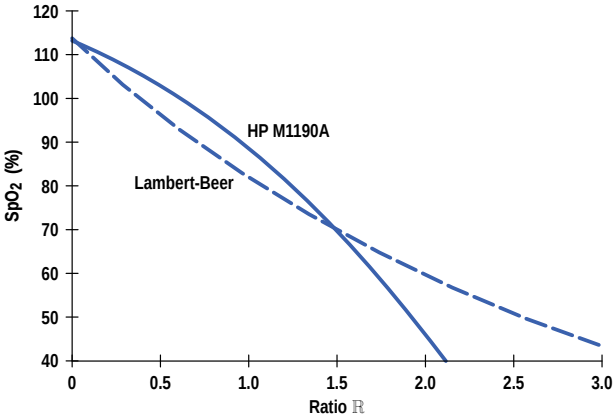

Fig. 9. *Theoretical (Lambert-Beer) and real calibration (arterial blood samples) curve for the HP M1190A adult sensor. The difference is mainly caused by scattering effects and nonideal light sources.*

Fig. 10 shows the sensor LED driver circuit and receiver circuit. The LEDs are driven in sequence at a repetition rate of 375 Hz in antiparallel fashion. At the photodiode the intensities arrive in the sequence red (R), infrared (IR) and dark. In the receiver circuit this signal is split into three paths: a red path, an infrared path, and a dark path. The dark intensity is subtracted from the red and infrared.

Fig. 11 shows the separated red and infrared patient signals with their I_{min} and I_{max} values caused by arterial pulsation, from which the ratio $\mathbb{R}$ can be calculated (equation 6).

Ambient Light and Electrical Noise

In a clinical environment, the sensor picks up ambient light and electromagnetic noise from various sources. The major source for ambient light is room illumination, typically fluorescent ceiling lamps, which have broad spectral bands with peaks at harmonics of the power-line frequency, 50 Hz or 60 Hz. Very often, electrical noise also comes from the power line and shows up as harmonics of the line frequency. Other well-known sources of large interfering electrical signals are the electrosurgery devices used in operating rooms, which can be very broadband.

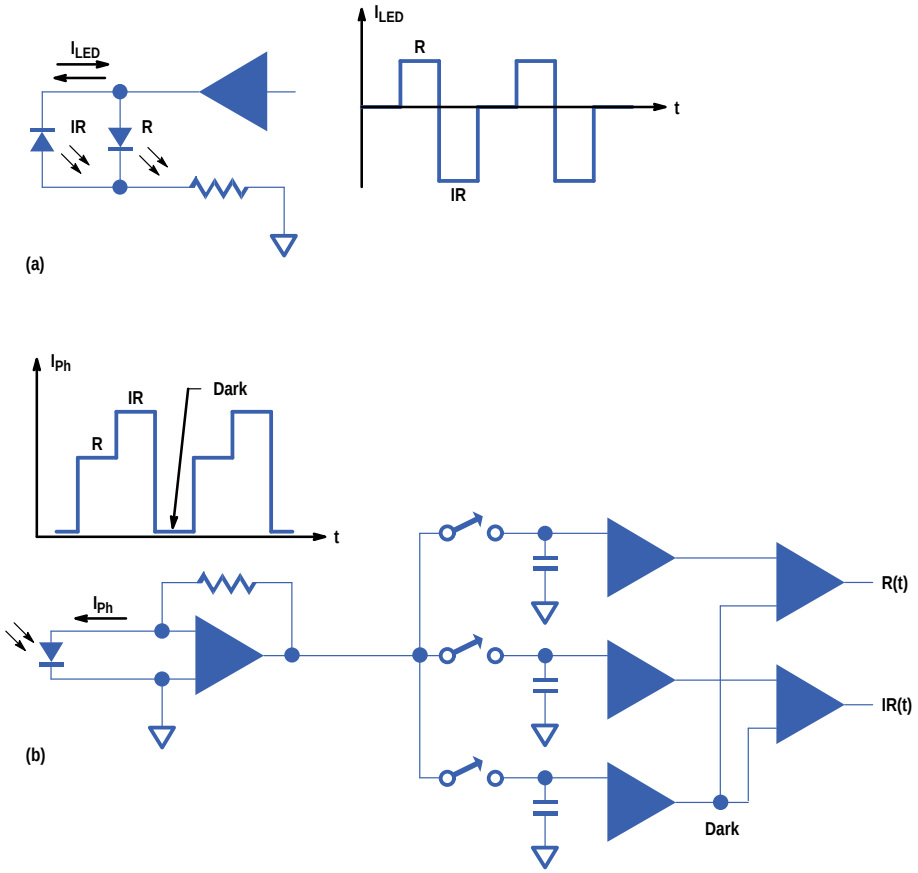

Fig. 10. *(a) Sensor LED driver circuit and (b) receiver circuit.*

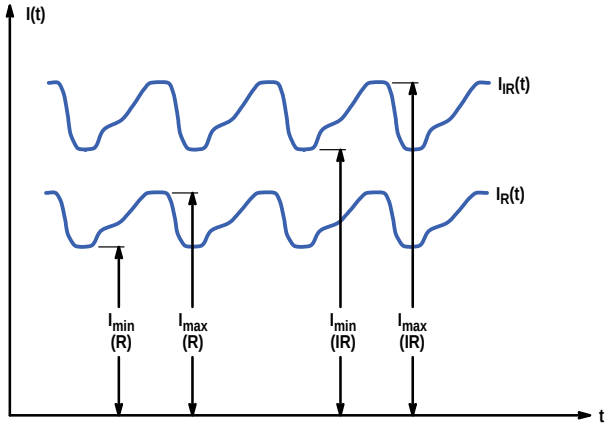

Fig. 11. *Separated red and infrared patient signals with their I_{min} and I_{max} values caused by arterial pulsation.*

Typical current levels at the sensor photodiode are around 1 μA dc with the blood current pulse modulated on the dc levels at a modulation depth of typically one percent. It is likely that the LED spectra including the desired signal and the optical or electrical noise spectra will overlap. Any noise lines in one of the LED modulation bands will be demodulated and folded down to the baseband, where they will contribute to poor signal-to-noise ratio (S/N). A very dangerous situation for the patient can occur in the monitoring of neonates, who are often treated with very bright UV lamps for bilirubin phototherapy. Neonates give poor SpO_2 signals because of poor vascular perfusion, so the bright UV ambient light can cause situations in which $S/N < 1$. A pulse oximeter is very likely to be misleading in these situations. It can derive values for pulse rate and oxygen saturation that are wrong because the input signals are dominated by noise.

Because interference can lead clinicians to apply incorrect care and therapy and cause harm or even death to patients, it must be avoided at all costs. A major goal for the sensor design was optimum optical and electrical shielding. Fig. 12 shows the pediatric sensor. Its closed housing is designed to shield the sensor from interfering ambient light.

Fig. 12. *The HP M1192A pediatric sensor has a closed housing to shield it from interfering ambient light.*

Movement Artifacts

Because the pulse oximetry method relies on the pulsatile part of the absorption, probably the most frequent cause of trouble is movement of the patient. Any movement usually causes movement of the sensor or the nonarterial tissue under the sensor and thereby leads to noise on the signals. A design goal for the new sensors was to be small and lightweight and to attach firmly to the patient. The cable was made as thin and flexible as possible consistent with the need for robustness, so that it adds little weight and stiffness, thereby helping to decouple the sensor from cable movements.

Cable Robustness

The clinical environment can be very harsh. Sensors fall off patients. People step on them and carts roll over them. Cables get squeezed between drawers and racks. The cables of medical sensors, in particular, have to be extremely robust. They are moved, bent, kinked, and treated with aggressive disinfectants.

A carefully selected lead composition and the use of nonbreakable material were goals for the cable construction. A new connector and interconnection concept are used. The interconnection is split into two parts: a short, thin, and more fragile cable is used with the sensors for low weight and minimum mechanical stiffness, while a longer, heavier, more robust cable was designed as an interface cable to the instrument.

The connector joining the cables (Fig. 13) is optimized for small size, low weight, and robustness. Special care was taken to provide very high insulation between the pins and to make the interconnect junction watertight to avoid leakage currents in humid environments like neonatal incubators. In older designs, saturated water vapor and salty residues from infusions or blood on connectors was a common source of problems, leading to erroneous measurement results.

Setting Design Goals

HP has offered a reusable SpO_2 sensor since 1988, but in one size only: the adult HP M1190A sensor. This sensor is very well-accepted. The objective for the new sensor project was to extend this sensor technology to a family of sensors covering all of the different application areas, so the customer is not forced to use a third-party sensor for application reasons.

(a) (b)

Fig. 13. *Plug and socket connector system.*

Based on experience with the HP M1190A sensor and on customer feedback we defined the following objectives:

- "Must" Objectives
  - Reusable sensors only
  - Cost competitive with disposable sensors
  - Clear, nonconfusing application
  - No burns on skin
  - State-of-the-art necrosis factor behavior (minimal local cell damage)
  - No penumbra effect
  - Influence of ESI (electrosurgery interference) as low as in HP M1190A
  - Backward compatibility with HP monitors (hardware)
- "Want" Objectives
  - Reliability equal to HP M1190A
  - Easy to use
  - Comfortable application over long period of time (several days)
  - Reliable fixing mechanism
  - Cleaning and sterilization by immersion in solutions
  - Mechanically robust design like HP M1190A
  - Cable size, length, flexibility, and quality similar to HP M1190A; alternatively, trunk cable and sensor cables
  - No influence of ambient light (operating room, bilirubin therapy, fluorescent lights)
  - Minimum motion artifacts
  - Backward compatibility with HP monitors (software)
  - Compatibility with competitive monitors.

Reusability was required because HP feels environmentally responsible for HP products. Most of the sensors on the market are disposable, which means that they are applied only once, after which they must be disposed of as medical waste. Reusable sensors are a small contribution to protecting the environment.

We used the Quality Function Deployment[3,4] (QFD) tool for developing these sensors. The starting point for QFD is the customer—what does the customer want? The customer requirements are weighted according to their relative importance, the corresponding engineering characteristics are listed, and step by step a matrix is built that provides the means for interfunctional planning and communication.

The three most important customer attributes we found are:

- Functionality. Minimize physiological effects like skin irritation and low perfusion. This means selecting the appropriate material and applying the appropriate clamping force.
- Performance. Ensure good signal quality. The most important issue was to select optical components to provide good light transmission.
- Regulations. The sensors had to meet U.S. FDA requirements and international safety and EMC standards.

We have had several clinical trials to verify that we understood the customer requirements correctly. At the release of the product for manufacturing we checked our solutions again to make certain that they are in accordance with the required customer attributes and engineering characteristics. We have been shipping the sensors for over half a year without any customer objections. This makes us fairly confident that the sensors meet customer expectations.

Design Concept

The next step after defining the project goals was to evolve the basic design concept. To reduce waste (even reusable parts have to be replaced eventually) we decided that each transducer would consist of two parts: an adapter cable to be used for all sensors and a sensor cable consisting of connector, transmitter, receiver, and a special sensor housing for the specific application site (finger of a child or small adult, foot or hand of a neonate, ear of an adult). We made this split since the lifetime of the adapter cable is longer (we estimated three times longer) than that of the sensor cable, which is much lighter in weight to reduce motion artifacts. A further advantage of the two-part design is the flexibility for future products to use the sensor without an adapter cable. The design required the development of a new 8-pin connector family.

To minimize the risk, because of the very good customer feedback for the existing adult sensor, we decided to change only the optical elements of the transducer.

The detailed design concept is shown in Fig. 14. The adapter cable is a shielded twisted-pair cable with four single conductors, a 12-contact male plug on the instrument side, and an 8-contact female connector on the sensor side. The sensor cable is a shielded twisted pair cable with two conductor pairs, an 8-contact male plug on the instrument side, a transducer consisting of transmitter and receiver molded in epoxy, and a special sensor housing.

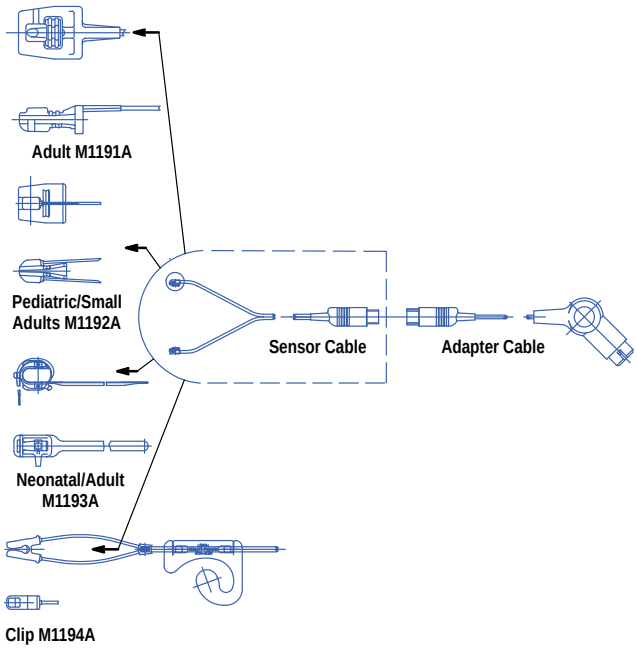

Fig. 14. *Design concept for the new sensor family.*

Housing

With the project goals in mind, the first proposals for the sensor housing were designed and prototype tooling was ordered to get parts ready for the first application tests. It was especially necessary to start with application tests as soon as possible for the neonate sensor, because this sensor would cover the biggest area and would be the most sensitive. The design of the pediatric sensor was more straightforward. It had to be similar to the existing adult sensor. For the other two sensors we approved a couple of proposals and ordered the prototype tooling for those.

With these samples we went into hospitals and spoke to nurses and medical technicians. When their response was positive, we began to improve the design step by step, making all changes in the prototype tooling as far as possible. If it was not possible to realize a necessary change, new prototype tooling was ordered. Only after this iterative process was complete did we order the final tooling.

The idea for the neonatal sensor, Fig. 15, was to place the transducer elements facing one another to make it easier to apply the sensor on foot or hand, and to have a long strap with a special fastener that allows application of the sensor on different foot or hand sizes. The transducer is positioned on the foot or the hand and the strap is threaded through the first latch and pulled slightly while holding the top of the transducer. The second latch is only used if the strap is too long.

The idea for the clip sensor was to integrate the spring for the necessary clamping force into the molded part (Fig. 16). The transducer is clipped onto the fleshy part of the earlobe. To minimize motion artifacts generated by patient movements a plastic fixing mechanism that hooks over the ear is provided.

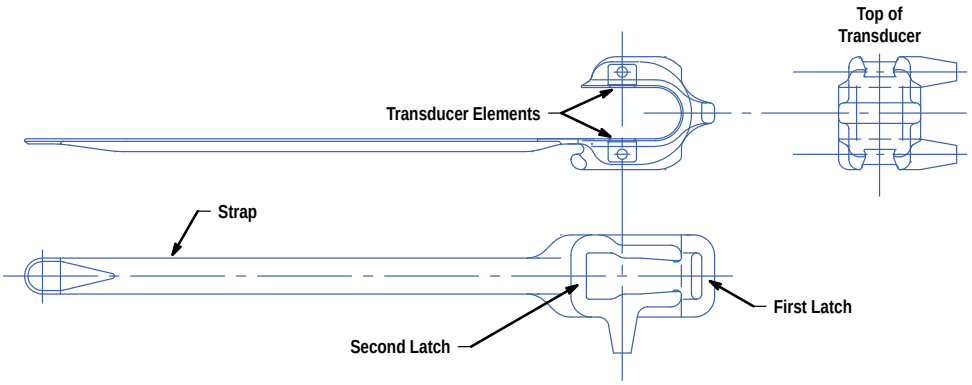

Fig. 15. *Neonatal sensor.*

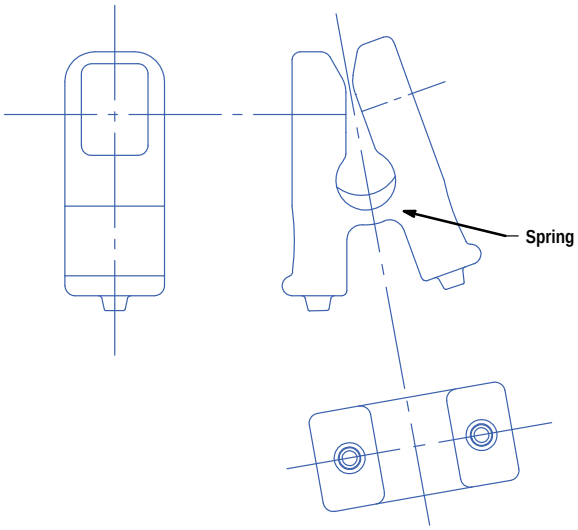

Fig. 16. *Clip sensor.*

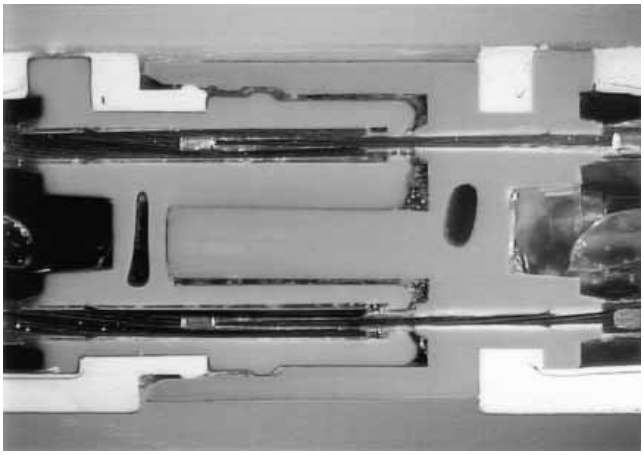

Fig. 17. *Cutaway view of two pins of the 8-pin connector between the adapter cable and the sensor cable. The connector is watertight when joined.*

Cable and Connector

Three different types of cables are used for the sensor family. For the adapter cable we use a very robust cable with an outer jacket made of polyurethane. The same adapter cable is used with all of the sensor types.

Two different sensor cables are used, one for the adult transducer and another for the rest of the family. They differ only in the outer jacket. For the adult sensor the outer jacket is made of silicone because of the manufacturing process. The sensor housing, which is made of silicone, is molded together with the cable and other elements in a molding machine. Because silicone can't be combined very well with different materials, the outer jacket must also be silicone.

For the rest of the sensor family we use a split, lightweight cable with an outer jacket made of polyurethane.

The construction of all three cables is similar. All are twisted-pair and have a Kevlar braid anchored in both the sensor and the connector to improve the strain relief.

The 8-pin connector between the sensor cable and the adapter cable also has a soft outer jacket made of polyurethane. The Kevlar braid is anchored inside the connector. Watertightness is achieved when the two halves of the connector are joined (see Fig. 17).

Optical Components

The optical elements are mounted on ceramic substrates shaped by cutting with a high-energy laser. The transmitter (Fig. 18) consists of two LED die (red and infrared) mounted on gold metallization. A photodiode on the receiver ceramic (Fig. 19) receives the sensor signal. A dome of epoxy material protects the elements and bond wires from mechanical stress. The wires of the transducer and the Kevlar braid are soldered and anchored on the backside of the ceramic.

To a first approximation, LEDs have a Gaussian intensity spectrum in which the peak wavelength is equal to the centroid wavelength. Because the red area (< 650 nm) of the extinction coefficients is very sensitive to wavelength variation (see Fig. 8) and the intensity distribution is not actually Gaussian and symmetrical, we use the centroid wavelength, which differs slightly from the peak wavelength, as an adequate characterization parameter for the LED (Fig. 20). Normally the

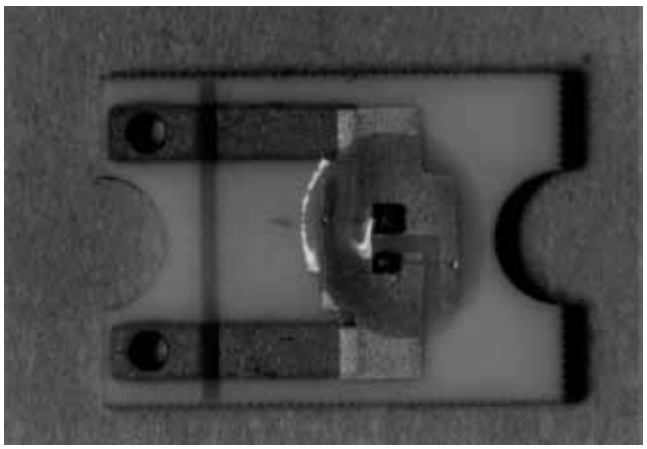

Fig. 18. *LED transmitter.*

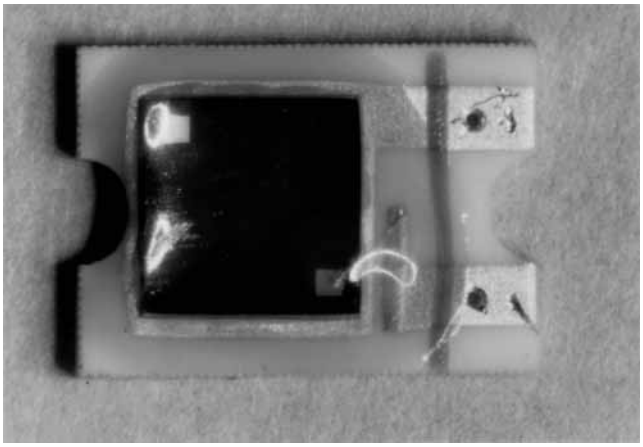

Fig. 19. *Photodiode receiver.*

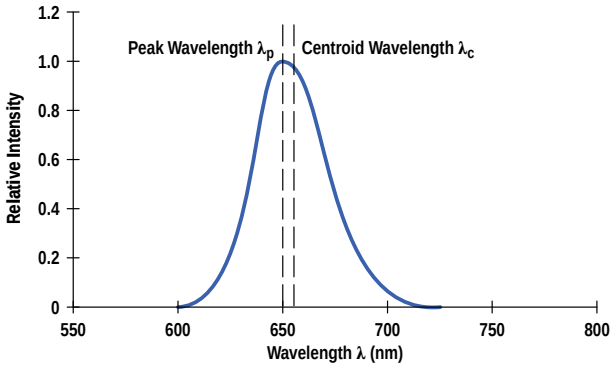

Fig. 20. *A typical LED intensity distribution. For SpO_2 measurements the centroid wavelength gives a better characterization than the peak wavelength.*

wavelength variation on a preselected wafer for red LEDs is in the range of ±5 nm. For the HP M1190A sensor in 1990, the HP Optoelectronics Division installed a selection process for a narrow, ±1-nm centroid wavelength variation.

For the new sensor family we chose for each sensor an LED pair with centroid wavelengths of 660 nm (red) and 890 nm (infrared). For the red LED a new high-efficiency AlGaAs technology was chosen. The maximum intensity for these LEDs is about a factor of four higher than for the older ones. This has the big advantage that the transmission values for both the red LEDs and the infrared LEDs are about the same. The average drive current for the LEDs, and therefore the heat dissipation, can be dramatically lowered.

The *transmission* Tr is defined as the ratio of photocurrent to LED current:

$$\mathrm{Tr} = \frac{I_{ph}}{I_{LED}}, \qquad (8)$$

where I_{ph} is in nanoamperes and I_{LED} is in milliamperes. Tr depends strongly on the absorption and extinction coefficients of the patient's tissue. Mean values are about 70 nA/mA over a large patient population. For thin absorbers like the earlobe, values of Tr as high as 300 nA/mA are possible. With new SpO_2 front-end hardware this would not have been a problem, but to be compatible with older pulse oximetry instruments we use a smaller active area of the photodiode for the HP 1194A ear sensor to get the same Tr values as the other sensors.

The LED supplier (not HP for the new sensors) guarantees a narrow centroid wavelength variation of less than ±2 nm. For LED qualification measurements, an optical spectrum analyzer with a wavelength resolution of 0.2 nm is used. All LED parameters are measured with a constant drive current of 20 mA. Because there is a wavelength shift over temperature of about 0.12 nm/K, the ambient temperature has to be held constant. Depending on the LED packaging, there is also a certain warmup time, which has to be held constant for LED qualification. In clinical practice, there can always be a temperature shift during SpO_2 measurements, but because of the definition of the ratio $\mathbb{R}$, with red intensity in the numerator and infrared intensity in the denominator (see equation 6), this effect is compensated within the specified operating temperature range of $15°C < T < 45°C$.

Another important factor is that some red LEDs have a low secondary emission (<4% of maximum intensity) at a wavelength of typically 800 to 850 nm (Fig. 21). For higher secondary intensities, interference with the infrared LED causes a ratio error and therefore an SpO_2 error, which must be eliminated. For the new high-efficiency LEDs the secondary emission is typically less than 0.1%.

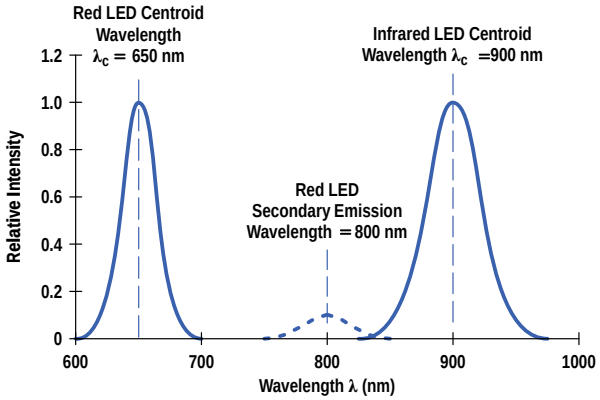

Fig. 21. *Typical red and infrared LED spectra for SpO_2 sensors. The spectral half-bandwidth for the red LED is about 20 nm and for the infrared LED about 40 nm. A secondary emission peak for the red LED is undesired and has to be lower than 4% of the maximum intensity.*

The receiver element is a standard silicon photodiode with peak sensitivity at 850 nm. The active area is approximately 2 mm square for the HP M1191/92/93A sensors and 1 mm square for the HP M1194A ear sensor. The die are mounted on a ceramic substrate with metalized layers for shielding.

The package for the LEDs in the HP M1190A sensor was a standard subminiature package. The emitter consisted of a red-infrared-red triplet in a longitudinal arrangement to make the apparent emission points for the red and infrared sources virtually identical. This is important for the ratio calculation, because both light paths have to be about the same length. One disadvantage is a possible malfunction when the patient's finger does not cover the entire light source. Then a part of the red light can cause an optical shunt that yields dc red levels that are too high (penumbra effect), causing false high readings. In the new sensor design, the two LEDs are very close together (<0.5 mm) on a common leadframe (see Fig. 22). This should eliminate the penumbra effect.

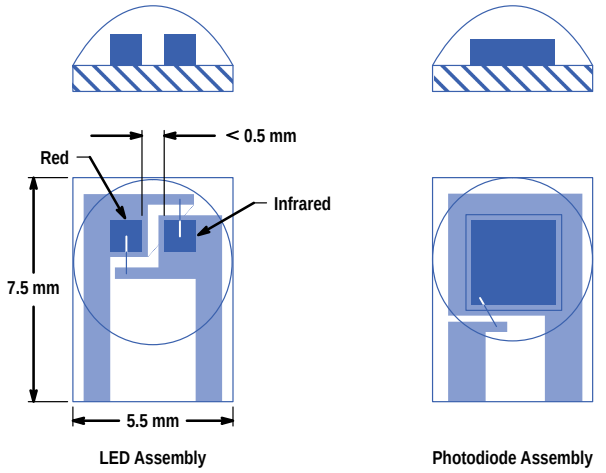

Fig. 22. *Transmitter and receiver assemblies for the new sensor family are on ceramic substrates. To avoid asymmetric optical shunting (penumbra effect) the two LED die are mounted as close as possible to each other. An epoxy coating is added before final packaging to protect the optical parts.*

The die are mounted on a ceramic substrate and covered with a transparent epoxy material. A design goal was to get a water and disinfectant resistant seal between the cable and the package. Immersion and disinfection tests show that this goal was achieved.

Materials

For the pediatric and neonatal sensors we chose silicone with a hardness of 35 ± 5 Shore A. The material is very robust and has good tensile strength compared to other silicones. Silicone is very often used in clinical areas and is very well-accepted. It is very resistant to chemicals and causes no skin irritations when used correctly.

For the clip sensor we chose a polyurethane with a hardness of 75 ± 5 Shore A, which gives the required clamping force (Fig. 23).

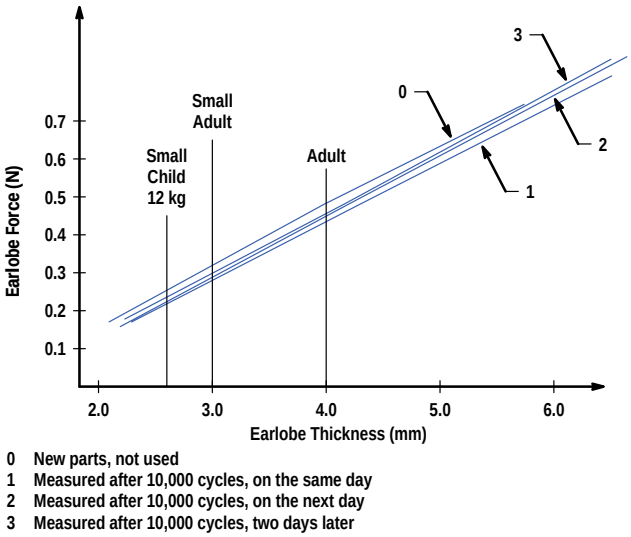

Fig. 23. *Spring forces in the clip sensor.*

Manufacturing Process

The manufacturing process for the new HP M1191A sensor is injection molding, the same as for the older HP M1190A. These sensors use only silicone rubber. For the HP M1192/ 93/94A sensors a different manufacturing process was necessary because these sensors use two different materials—silicon rubber and polyurethane, which do not combine well in the injection molding process. We also wanted to reduce the manufacturing costs and to gain more flexibility in choosing suppliers.

We decided to cast the premounted optical elements together with the cable in a special epoxy that combines very well with the cable including the Kevlar braid. We thus ensured watertightness, which means the sensors can be disinfected by immersion in solutions.

Reliability

To reach the reliability goals a few iterative changes were necessary and different tests installed. Many tests and customer visits were conducted to ensure that the sensors will not break. We tested several housing materials until we found the right one for the rough clinical environment. The tensile strength and robustness have been improved dramatically compared to the first samples. The method of anchoring the Kevlar braid in the ceramic substrate and connector was also improved several times. Every prototype was tested in the same way, by a combination of mechanical stress and cleaning by immersion in different solutions.

Technical Qualification

The most important factor for qualifying the new SpO_2 sensors has been how to determine test methods that are able to expose any weak points of the design. The qualification stress should be higher than the normal clinical application stress to provoke failures. The fulfillment of customer expectations concerning reliability was the overall guideline for prioritizing the test emphasis. Because of its customer orientation, the QFD methodology was an excellent tool for determining the main focus for testing. To make QFD more practical, we divided the sensor into three subelements, which made the specifics of the subassembly more visible. The three subelements were the interconnection, the sensor housings, and the optical assemblies.

The correlation matrix between the customer requirements and the technical specifications generated a relative importance ranking within the broad list of requested technical details. We could now determine which were the most important technical parameters. Their performance would have the greatest impact on the acceptance of the sensors in the market.

It was very important to assess the technical complexities and difficulties in the realization of technical specifications. This was the task of the engineers of a crossfunctional team chosen for their experience and ability to foresee potential problems. The correlation between expected technical difficulties and the importance of the parameters to the customer was an

essential input for further activities. We could now focus our efforts to reduce the risk potentials, which were clearly defined. High risk means high importance correlated with high technical difficulty ratings. These high-priority items were communicated to the project managers to give them an impression of the degree of technical maturity in this early project phase.

A critical assessment of design risk potential could now be made. This triggered a review of the importance of each customer requirement and gave the designers valuable inputs for design concepts. The results were also useful when considering strategies for accelerated stress testing.

The next step in the QFD process was to transfer the information on high-priority technical requirements into another matrix showing the relationship between parts characteristics and technical requirements. The key deliverables of this exercise were:

- Identification of key parts and their characteristics
- Preselection of parts characteristics to find critical parts for performing a design failure mode and effect analysis (FMEA)
- Information to aid in selecting between design alternatives to find the most competitive design concepts
- Inputs for stress testing using parts characteristic importance information.

The FMEA generates risk priority numbers (RPN). These numbers describe how often a failure will be occur, how easily it will be detected, and how severe the failure will be. Taking the interconnection as an example, the risk assessment was divided into three categories:

- High Risk: RPN > 200 and high parts importance
- Medium Risk: RPN > 100 and high parts importance
- Low Risk: RPN > 100 and low parts importance.

In this way, key customer needs were identified and test parameters selected. We also took into account the feedback from clinical trials.

Fig. 24 gives an overview of the qualification tests that were performed to get release approval for the sensors. A special machine was designed to simulate the cable stress that occurs in hospitals. We call this test the bending/torsion test. With a calculated number of cycles, equivalent to our reliability goals, we stressed the critical cable sections to ensure that the lifetime requirements were met.

Supplier Selection

The supplier chosen to manufacture the new SpO_2 sensor family had to meet a number of specific requirements. The supplier is responsible for the majority of the manufacturing process steps. This has a positive influence on production lead time, logistics, communication, and costs. To reach our quality goals with one supplier who is responsible for nearly all process steps is much easier than with a long chain of suppliers. The requirements covered technology, vertical integration, and costs.

Fourteen international suppliers were evaluated. Nine were not able to manufacture the sensors because they did not have the required technology. After considering cost aspects, only two suppliers fulfilled the selection criteria. For these two suppliers, we constructed supplier profiles derived from the QFD method.

To construct a profile, each customer need is listed along with an evaluation of how well the supplier fulfills that need in terms of technology and processes. The level of fulfillment is evaluated by an HP specialist team, which also evaluates the importance of each customer need. The profile shows the supplier's strengths and weaknesses and gives a point score. The supplier with the higher number of points is considered better qualified to manufacture these products.

To evaluate critical technology and processes, design and process failure mode and effect analyses (FMEAs) were conducted for both suppliers' products. To evaluate each manufacturer's capabilities, a quality and process audit was performed at the manufacturing site. The auditors reviewed the site and manufacturing processes for comparable products that were identified as critical for our sensor products.

Production Wavelength Measurements

The measurement of LEDs for the SpO_2 sensors at the manufacturing site is a critical and sensitive manufacturing process step. To guarantee the accuracy of HP SpO_2 measurements the wavelength of the red LED has to be within a very small range: between 657 and 661 nm. To measure the LED wavelength a very accurate optical spectrometer is used. To obtain repeatable measurement results, an integrating sphere is used to couple the light of the red LED into the spectrometer (see Fig. 25).

An integrating sphere is a ball with a highly reflective surface. The light is reflected many times on the surface and becomes diffuse. As a result, the spectrum and the intensity of an LED are the same at each point of the surface of the ball and can be coupled easily into the spectrometer. The main advantage of this method is that tolerances in the placement of the LED are

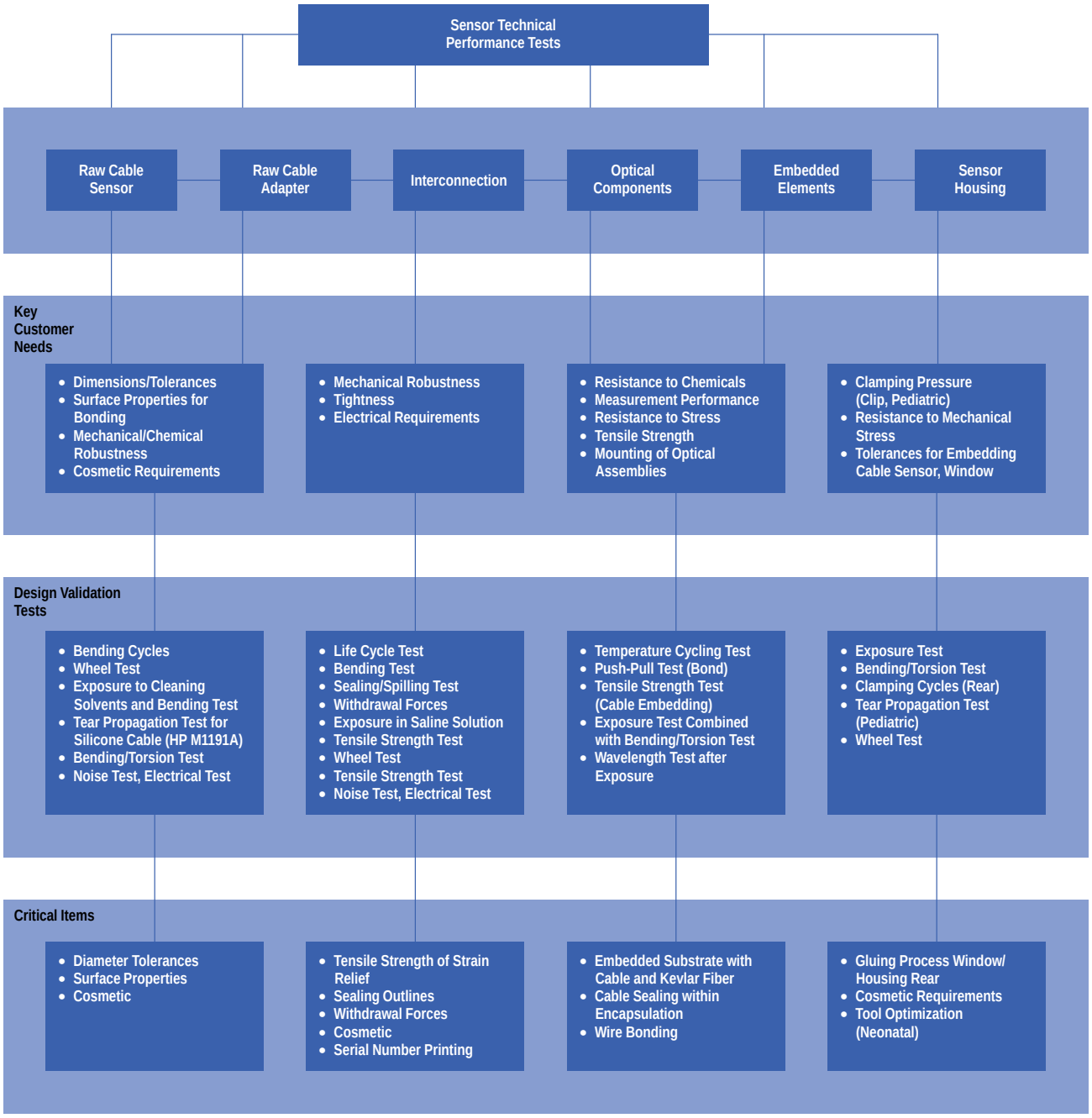

Fig. 24. *Qualification tests for the new sensor family.*

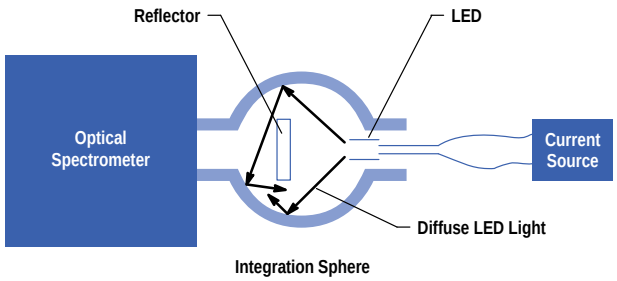

Fig. 25. *Setup for LED spectral measurements.*

not critical and the repeatability is very good compared to other methods. Fig. 26 shows a typical spectrum of a red LED measured with an integration sphere.

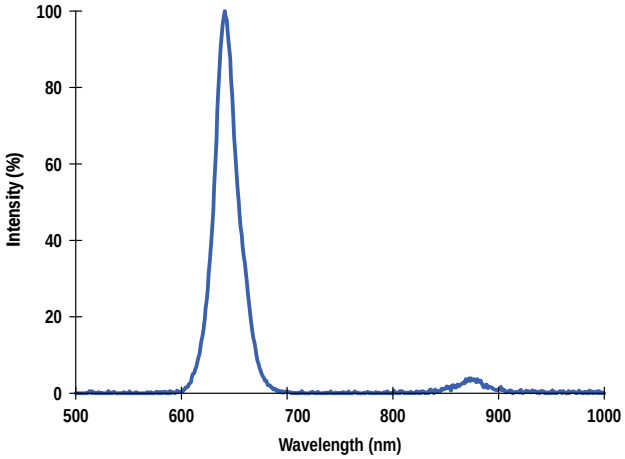

Fig. 26. *Spectrum of a red LED measured with an integration sphere.*

There are different ways to measure the wavelength of an LED. One is the peak wavelength, which is the highest point of the spectrum. The centroid wavelength, which is used in our measurements, calculates the center of the area under the spectrum. A secondary peak in the spectrum of the LED can have a large influence on the measurement results and has to be very small ($< 1\%$).

The temperature of the LED die has a large influence on the emitted wavelength—the higher the temperature the higher the wavelength (0.12 nm/K). Therefore, the LED must be in thermal equilibrium. In practice, the LED takes only a few seconds to reach thermal equilibrium. The ambient temperature must be monitored and if the temperature changes the spectrometer must be recalibrated.

Summary

A new family of reusable pulse oximetry sensors has been developed. Based on the HP M1190A, HP's first reusable SpO_2 sensor, these sensors can noninvasively monitor the blood oxygen levels of patients, a key vital sign. They are used primarily in operating rooms, recovery rooms, intensive-care units, and some general wards. The new sensor family covers all application areas and consists of the M1194A clip sensor (Fig. 27), the HP M1191A adult sensor with new wavelength (Fig. 28), the HP M1192A pediatric sensor (Fig. 12), and the HP M1193A neonatal sensor (Fig. 29).

Acknowledgments

Many people were involved in this project. The authors would especially like to thank Dietrich Rogler for the industrial design of the sensors, Willi Keim and Peter Jansen of materials engineering for their excellent support, Martin Guenther for performing all the optical characteristics measurements, Gerhard Klamser for verifying the algorithm, Gerhard Lenke for organizing all the regulation tasks, and Otto Gentner for managing the clinical trials. Special thanks to Professor Dr. J. W. Severinghaus of the University of California Hospital in San Francisco for performing volunteer studies.

Fig. 27. *HP M1194A clip sensor.*

Fig. 28. *HP M1191A adult sensor.*

Fig. 29. *HP M1193A neonatal sensor.*

References

1. T.J. Hayes and E.B. Merrick, "Continuous, Non-Invasive Measurements of Blood Oxygen Levels," *Hewlett-Packard Journal*, Vol. 28, no. 2, October 1976, pp. 2-10.
2. *Hewlett-Packard Journal*, Vol. 42, no. 4, October 1991, pp. 6-54.
3. D. Clausing, "The House of Quality," *Business Review*, May-June 1988.
4. L.P. Sullivan, "Quality Function Deployment," *Quality Progress*, June 1986, pp. 39-50.

▶ Go to Subarticle 7a

▶ Go to Subarticle 7b

▶ Go to Next Article

▶ Go to Journal Home Page